

## EXPLOSIVE NUCLEOSYNTHESIS IN ASPHERICAL HYPERNOVA EXPLOSIONS AND LATE TIME SPECTRA OF SN1998BW

KEIICHI MAEDA<sup>1</sup>, TAKAYOSHI NAKAMURA<sup>2</sup>, KEN'ICHI NOMOTO<sup>3,7</sup>, PAOLO A. MAZZALI<sup>4,7</sup>,  
 FERDINANDO PATAT<sup>5</sup>, IZUMI HACHISU<sup>6</sup>

*Submitted to the Astrophysical Journal Letters on 9 October 2000*

### ABSTRACT

Aspherical explosion models for the hypernova (hyper-energetic supernova) SN 1998bw are presented. Nucleosynthesis in aspherical explosions is examined with a two-dimensional hydrodynamical code and a detailed nuclear reaction network. The nebular line profiles of the Fe-dominated blend near 5200 Å and of O I] 6300,6363 Å are calculated and compared with the observed late time spectra of SN 1998bw. Compared with the spherical model, the unusual features of the observed nebular spectra can be better explained if SN 1998bw is a strongly aspherical explosion with a kinetic energy of  $\sim 10^{52}$  ergs viewed from near the jet direction. The strongly aspherical explosion model might also be able to reproduce the slowly declining tail of the light curve of SN 1998bw at late times and to explain the connection with GRB980425.

*Subject headings:* supernovae: individual: SN1998bw — gamma rays: bursts — nucleosynthesis — line: profiles

### 1. INTRODUCTION

SN 1998bw was discovered as the optical counterpart of GRB980425 (Galama et al. 1998), and it was soon recognized as an unusually bright and energetic Type Ic supernova (SN Ic). The light curve and the unusual spectra of SN 1998bw at early times have been successfully modeled with a hyper-energetic explosion (kinetic energy  $E \sim 4 \times 10^{52}$  ergs) of a massive C+O star (Iwamoto et al. 1998; Woosley, Eastman & Schmidt 1999; Branch 2000). In this paper the term "hypernova" is used to refer to a hyper-energetic SN explosion with  $E \geq 10^{52}$  ergs, without specifying the nature of the central engine.

Despite the success of the hypernova model in reproducing the observed features of SN 1998bw at early times, some properties of the observed light curve and spectra at late times are difficult to explain in the context of a spherically symmetric model. (1) The decline of the observed light curve tail is slower than that of the synthetic curve, indicating that at advanced epochs  $\gamma$ -ray trapping is more efficient than expected (Nakamura et al. 2000a; Sollerman et al. 2000). (2) The widths of the nebular emission lines suggest that the mean expansion velocity of iron is higher than that of oxygen and that a significant amount of oxygen exists at low velocity (Danziger et al. 1999; Nomoto et al. 2000; Patat et al. 2000; Sollerman et al. 2000). Both these features are in conflict with what is expected from a spherically symmetric explosion model, where  $\gamma$ -ray deposition is a decreasing function of time

and where iron is produced in the deepest layers and thus has a lower average velocity than oxygen. We suggest that these are signatures of asymmetry in the ejecta. Therefore in this paper we examine aspherical explosion models for hypernovae.

On the theoretical side, aspherical explosions of massive stars have been investigated as possible sources of  $\gamma$ -ray bursts. Woosley (1993) and Paczynski (1998) suggested that the collapse of massive stars can give rise to  $\gamma$ -ray bursts. MacFadyen & Woosley (1999) showed numerically that the collapse of a rotating massive core can form a system consisting of a black hole and an accretion disk, and that a jet emerges along the rotation axis following the input of energy from accretion onto the black hole. The jet can produce a highly asymmetric supernova explosion if its lateral expansion transfers a sufficient amount of energy from the jet to the surrounding stellar envelope (Khokhlov et al. 1999). However, these studies did not calculate explosive nucleosynthesis. Moreover, spectroscopic and photometric features of aspherical explosions have not been shown in these earlier studies. Nagataki et al. (1997) performed two-dimensional nucleosynthesis calculations for aspherical supernova explosions to explain some features of SN 1987A, but they only addressed the case of a normal explosion energy.

In the present study, we examine the effect of aspherical (jet-like) explosions on nucleosynthesis in hypernovae. We then investigate the degree of asphericity in the ejecta of

<sup>1</sup>Department of Astronomy, School of Science, University of Tokyo, 7-3-1 Hongo, Bunkyo-ku, Tokyo 113-0033, Japan ; maeda@astron.s.u-tokyo.ac.jp

<sup>2</sup>Department of Astronomy, School of Science, University of Tokyo, 7-3-1 Hongo, Bunkyo-ku, Tokyo 113-0033, Japan ; nakamura@astron.s.u-tokyo.ac.jp

<sup>3</sup>Department of Astronomy, School of Science, University of Tokyo, 7-3-1 Hongo, Bunkyo-ku, Tokyo 113-0033, Japan ; nomoto@astron.s.u-tokyo.ac.jp

<sup>4</sup>Osservatorio Astronomico di Trieste, via G. B. Tiepolo 11, I-34131 Trieste, Italy; mazzali@ts.astro.it

<sup>5</sup>European Southern Observatory, K. Schwarzschild Str. 2, D-85748 Garching b.München, Germany ; fpatat@eso.org

<sup>6</sup>Department of Earth Science and Astronomy, Collage of Arts and Science, University of Tokyo, Meguro-ku, Tokyo 153-0041, Japan ; hachisu@chianti.c.u-tokyo.ac.jp

<sup>7</sup>Research Center for the Early Universe, School of Science, University of Tokyo, Tokyo 113-0033, Japan

SN 1998bw, which is critically important information to confirm the SN/GRB connection, by computing synthetic spectra for the various models viewed from different orientations and comparing the results with the observed late time spectra (Patat et al. 2000).

## 2. MODELS

Our calculations are performed in two steps. The first step is a hydrodynamical simulation of the explosion with a two-dimensional Eulerian hydrodynamical code, which is based on Roe's scheme (Hachisu et al. 1992, 1994). We solve Euler's equations with a constant adiabatic index  $\gamma = 4/3$ , which is a good approximation if the pressure is radiation-dominated. The effect of nuclear reactions on the hydrodynamics is negligible since the explosion energy is large. The number of meshes is  $120 \times 120$  on a cylindrical ( $r, z$ ) coordinate system. The mesh sizes are linearly zoned and decrease inward, which enables us to achieve a high resolution of the hydrodynamic evolution of the central regions where explosive nucleosynthesis takes place.

In our calculations we follow a number of test particles, tracking their density and temperature history. The number of test particles is 190 for particles initially in the Si layer and 2250 for particles initially in the C+O layer. The particle histories are used in the second step to calculate the change in the chemical composition, using a reaction network including a total 222 isotopes up to  $^{71}\text{Ge}$  (Thielemann, Nomoto & Hashimoto 1996).

We construct several asymmetric explosion models (A-E) for various combinations of the model parameters, as summarized in Table 1. Details of the various models will be published elsewhere. The progenitor model is the  $16 M_{\odot}$  He core of a  $40 M_{\odot}$  star (Nomoto & Hashimoto 1988). The mass of the C+O core is  $13.8 M_{\odot}$ , which is the same as that used in Iwamoto et al. (1998) and Nakamura et al. (2000a, b). The explosion energies (i.e., final kinetic energies) are  $E = 1 \times 10^{52}$  ergs and  $3 \times 10^{52}$  ergs. We start the hydrodynamical simulation by depositing the energy below the mass cut that divides the ejecta from the collapsing core. We divide the deposited energy between thermal and kinetic energy, with various ratios. In order to generate the asymmetry, we distributed the initial kinetic energy in an axisymmetric way. In particular, we imposed different initial velocities below the mass cut in different directions:  $V_z = \alpha \times z$  in the jet direction and  $V_r = \beta \times r$  on the equatorial plane. The ratio  $\alpha/\beta$  ranges from 8:1 to 1:1 (spherical case). The mass cut is set at  $M_r = 2.4 M_{\odot}$ , so that the mass of  $^{56}\text{Ni}$  ejected is  $\sim 0.5 M_{\odot}$  to reproduce the peak of the light curve (Nakamura et al. 2000a).

## 3. NUCLEOSYNTHESIS

Figure 1 shows the isotopic composition of the ejecta of model C ( $E = 1 \times 10^{52}$  ergs, initial kinetic energy fraction 0.5, and  $\alpha/\beta = 8$ ) in the direction of the jet (upper panel) and perpendicular to the jet (lower panel). In the  $z$ -direction, where the ejecta carry more kinetic energy, the shock is stronger and post-shock temperatures are higher, so that explosive nucleosynthesis takes place in more extended, lower density regions compared with the  $r$ -direction. Therefore, larger amounts of  $\alpha$ -rich freeze-out elements, such as  $^4\text{He}$  and  $^{56}\text{Ni}$  (which decays into  $^{56}\text{Fe}$  via  $^{56}\text{Co}$ ) are produced in the  $z$ -direction than in the

$r$ -direction. Also, the expansion velocity of newly synthesized heavy elements is much higher in the  $z$ -direction. Comparison with the nucleosynthesis of spherically symmetric hypernova explosions (Nakamura et al. 2000b; Nomoto et al. 2000) shows that the distribution and expansion velocity of newly synthesized elements ejected in the  $z$ -direction in model C is similar to the result of the spherical explosion model with  $E \sim 3 \times 10^{52}$  ergs, although the integrated kinetic energy is only  $E = 1 \times 10^{52}$  ergs.

On the other hand, along the  $r$ -direction  $^{56}\text{Ni}$  is produced only in the deepest layers, and the elements ejected in this direction are mostly the products of hydrostatic nuclear burning stages (O) with some explosive oxygen-burning products (Si, S, etc). The expansion velocities are much lower than in the  $z$ -direction.

Figure 2 shows the 2-dimensional distribution of  $^{56}\text{Ni}$  and  $^{16}\text{O}$  in model C in the homologous expansion phase. In the direction closer to the  $z$ -axis, the shock is stronger and a low density,  $^4\text{He}$ -rich region is produced.  $^{56}\text{Ni}$  is distributed preferentially in the jet direction, but it is mostly located slightly off that direction because the shock propagates laterally (in the  $r$ -direction) as it penetrates the stellar envelope. As a result, the distribution of heavy elements is elongated in the  $z$ -direction, while the  $^{16}\text{O}$  distribution is less aspherical. On the other hand, densities in the  $r$ -direction are higher than in the  $z$ -direction, because the ejecta move slower in the  $r$ -direction, so that the density at a given radius is higher in the  $r$ -direction than in the  $z$ -direction.

Our results are qualitatively consistent with previous 2D calculations for SN 1987A (Nagataki et al. 1997). However, the amount of newly synthesized elements, especially  $^{56}\text{Ni}$ , is much larger, and the expansion velocities are much faster in our energetic models.

## 4. THE LATE TIME SPECTRA OF SN 1998BW

Mazzali et al. (2000) calculated synthetic nebular-phase spectra of SN 1998bw assuming spherical and uniform (i.e. fully mixed) ejecta. They showed that the nebular lines of different elements can be reproduced if different velocities are assumed for these elements, and that a significant amount of slowly-moving O is necessary to explain the zero velocity peak of the O I line. Different amounts of  $^{56}\text{Ni}$  ( $0.35 M_{\odot}$  and  $0.6 M_{\odot}$ , respectively) are required to fit the narrow O I line and the broad-line Fe spectrum (see figures in Danziger et al. 1999 and Nomoto et al. 2000). This suggests that an aspherical distribution of Fe and O may explain the observations.

In order to verify the observable consequences of an axisymmetric explosion, we calculated the profiles of two nebular lines for models A-E. One is the Fe-dominated blend near  $5200\text{\AA}$ , and the other O I]  $6300, 6363\text{\AA}$ . These are the lines that deviate most from the expectations from a spherically symmetric explosion. Line strengths were computed using line emissivities from a spherically symmetric NLTE nebular code, based on the deposition of  $\gamma$ -rays from  $^{56}\text{Co}$  decay in a nebula of uniform density, and the column densities of the various elements along different lines of sight as derived from the element distribution obtained from our 2D explosion models. The average electron density in the nebula is  $\log n_e = 7.47 \text{ cm}^{-3}$  (Danziger et al. 1999; Mazzali et al. 2000).

The nebular line profiles of iron and oxygen for model C

viewed at an angle of 15° from the jet direction are shown in Figure 3. In this figure, the observed spectrum on day 139 (Patat et al. 2000) is also plotted for comparison.

Table 1 gives the ‘full-width-at-half-maximum’ of the observed lines in SN 1998bw and of our synthetic lines. These should be compared to the observational values, which are 440Å for the Fe-blend and 200Å for the O I] doublet, and were estimated from the late time spectrum of 12 Sept 1998, 139 days after the explosion in the SN rest frame, assuming that the continuum level is the value around 5700 Å where the flux has the minimum value.

The observed line profiles are not explained with a simple spherical model. In a spherical explosion (model E) oxygen is located at higher velocities than iron, and although the Fe-blend can be wider than the O line if the O and Fe regions are mixed extensively, the expected ratio of the width of the Fe-blend to that of the O line in a spherically symmetric, fully mixed model is  $\sim 3 : 2$  (Mazzali et al. 2000). However, the observed ratio is even larger,  $\sim 2 : 1$ .

Our aspherical explosion models can produce a larger ratio than the spherical model (Table 1) because Fe is distributed preferentially along the jet direction. If we view the most strongly aspherical explosion model (A) from a near-jet direction, the ratio between the Fe and O line widths is comparable to the observed value (Table 1). For a larger explosion energy (model B), the width of the oxygen line is too large to be compatible with the observations.

When the degree of asphericity is high and the viewing angle is close to the jet direction, the component iron lines in the blend have double-peaked profiles, the blue- and red-shifted peaks corresponding to Fe-dominated matter moving towards and away from us, respectively. This is because Fe is produced mostly along the  $z$  (jet) direction. Because of the high velocity of Fe, the peaks are widely separated, making the blend wide. This is the case for the synthetic Fe-blend shown in Figure 3. In contrast, the oxygen line is narrower and has a sharper peak, because O is produced mostly in the  $r$ -direction, at lower velocities and with a less aspherical distribution.

The Fe-blend line computed with the aspherical model shows some small peaks (Fig. 3), which are not seen in the observations. Such small peaks are more pronounced for more asymmetric models. However, the detailed profile of the Fe-blend is very sensitive to the matter distribution. Mixing of the ejecta as suggested in the light curve model (Nakamura et al. 2000a) may distribute the fast-moving  $^{56}\text{Ni}$  over a wider range of velocities, which would reduce the double-peaked profiles of the Fe lines. Also, in the present work we have used a spherical, uniform density nebular model to compute line emissivities. In an as-

pherical model, dense central and equatorial regions may have higher  $\gamma$ -ray trapping efficiency, which may result in stronger low-velocity line emission than in our model (Fig. 2). Thus the component iron lines in the blend may have wider, flat-top profiles rather than double-peaked shapes, which could eliminate the minor peaks in the Fe blend seen in our present models. 2D  $\gamma$ -ray trapping calculations are therefore needed to compute the detailed spectra and the light curve.

## 5. CONCLUDING REMARKS

We calculated nucleosynthesis in aspherical hypernova explosions to compare with observations. We show that the unusual ratio of the width of the O and Fe nebular lines in SN 1998bw can be explained with a strongly aspherical explosion model viewed from a near-jet direction. Also, in this case the O line has a very sharp peak, in agreement with observations. Our results therefore confirm the suggestion that the nebular spectra of SN 1998bw carry the signature of an aspherical explosion (Mazzali et al 2000).

Our aspherical explosion models may be able to explain the slow decline of the late-time light curve of SN 1998bw. In these models, the region perpendicular to the jet is denser than in a spherically symmetric model having the same explosion energy. At very advanced epochs this region may be able to trap  $\gamma$ -rays more efficiently than a spherical model (Nakamura et al. 2000a).

Our strongly aspherical explosion model has an axis ratio of about 3:2 at the outer edge of the oxygen envelope (Fig. 2). This is consistent with the linear optical polarization of  $\sim 0.5\%$  observed in SN 1998bw (Kay et al. 1998; Iwamoto et al. 1998; Patat et al. 2000).

SN 1998bw was suggested to be physically connected with GRB980425. In spherical explosion models, the energy contained in the relativistic region is too small to induce even a weak  $\gamma$ -ray burst such as GRB980425 (Iwamoto et al. 1998; Woosley et al. 1999; Nakamura et al. 2000a). If SN 1998bw was a highly aspherical explosion viewed from near the jet direction it is more likely to have produced a  $\gamma$ -ray burst than if it was a spherical explosion, because most of the energy would be concentrated in the jet direction. We plan to perform calculations with much higher resolution near the surface than the present models to investigate whether the energy stored in relativistic region is enough to give rise to a GRB.

This work has been supported in part by the grant-in-Aid for COE Scientific Research (07CE2002, 12640233) of the Ministry of Education, Science, Culture, and Sports in Japan.

## REFERENCES

Branch, D. 2000, in “Supernovae and Gamma Ray Bursts” eds. M. Livio, et al. (Cambridge: Cambridge University Press), in press

Danziger, I.J., et al. 1999, in The Largest Explosions Since the Big Bang: Supernovae and Gamma Ray Bursts, eds. M. Livio, et al. (Baltimore: STScI), 9

Galama, T.J., et al. 1998, Nature, 395, 670

Hachisu, I., Matsuda, T., Nomoto, K., & Shigeyama, T. 1992, ApJ, 390, 230

Hachisu, I., Matsuda, T., Nomoto, K., & Shigeyama, T. 1994, A&AS, 104, 341

Iwamoto, K., et al. 1998, Nature, 395, 672

Kay, L.E., et al., 1998, IAU Circ., No.6969

Khokhlov, A.M., Höflich, P.A., Oran, E.S., Wheeler, J.C., Wang, L., & Chtchelkanova, A.Yu. 1999, ApJ, 524, L107

MacFadyen, A.I. & Woosley, S.E. 1999, ApJ 524, 262

Mazzali, P.A., et al. 2000, in preparation

Nakamura, T., Mazzali, P. A., Nomoto, K., & Iwamoto, K. 2000a, ApJ, submitted (astro-ph/0007010)

Nakamura, T., Umeda, H., Iwamoto, K., Nomoto, K., Hashimoto, M., Hix, R.W., & Thielemann, F.-K. 2000b, ApJ, submitted

Nagataki, S., Hashimoto, M., Sato, K., & Yamada, S. 1997, ApJ, 486, 1026

Nomoto, K., & Hashimoto, M. 1988, Phys. Rep., 256, 173

Nomoto, K., et al. 2000, in "Supernovae and Gamma Ray Bursts" eds. M. Livio, et al. (Cambridge: Cambridge University Press), in press (astro-ph/0003077)  
Paczynski, B. 1998, ApJ, 494, L45  
Patat, F., et al. 2000, ApJ, submitted

Sollerman, J., Kozma, C., Fransson, C., Leibundgut, B., Lundqvist, P., Ryde, F., & Woudt, P. 2000, ApJ 537, L127  
Thielemann, F.-K., Nomoto, K., & Hashimoto, M. 1996, ApJ, 460, 408  
Woosley, S.E., Eastman, R.G., & Schmidt, B.P. 1999, ApJ, 516, 788  
Woosley, S.E. 1993, ApJ, 405, 273

TABLE 1  
HALF LINE WIDTHS<sup>a</sup>

Model	$\alpha/\beta$	initial kinetic energy fraction	Final kinetic energy ( $10^{51}$ ergs)	Line Width (Å) <sup>b</sup>		
				(5 deg)	(15 deg)	(30 deg)
A	16	0.65	10	430 / 220	420 / 250	400 / 260
B	8	0.5	30	440 / 270	440 / 330	350 / 370
C	8	0.5	10	330 / 140	350 / 210	320 / 260
D	2	0.5	10	300 / 290	300 / 320	300 / 340
E	1	0.5	10	300 / 390	...	...

<sup>a</sup>Half line widths of the Fe-blend (near 5200Å) and of the O-doublet (6300,6363Å) for SN 1998bw. The observed values are 440 Å for the Fe-blend and 200 Å for the O-doublet.

<sup>b</sup>Fe width (Å) / O width (Å).

<sup>c</sup>Angle between the line of sight and the jet direction.

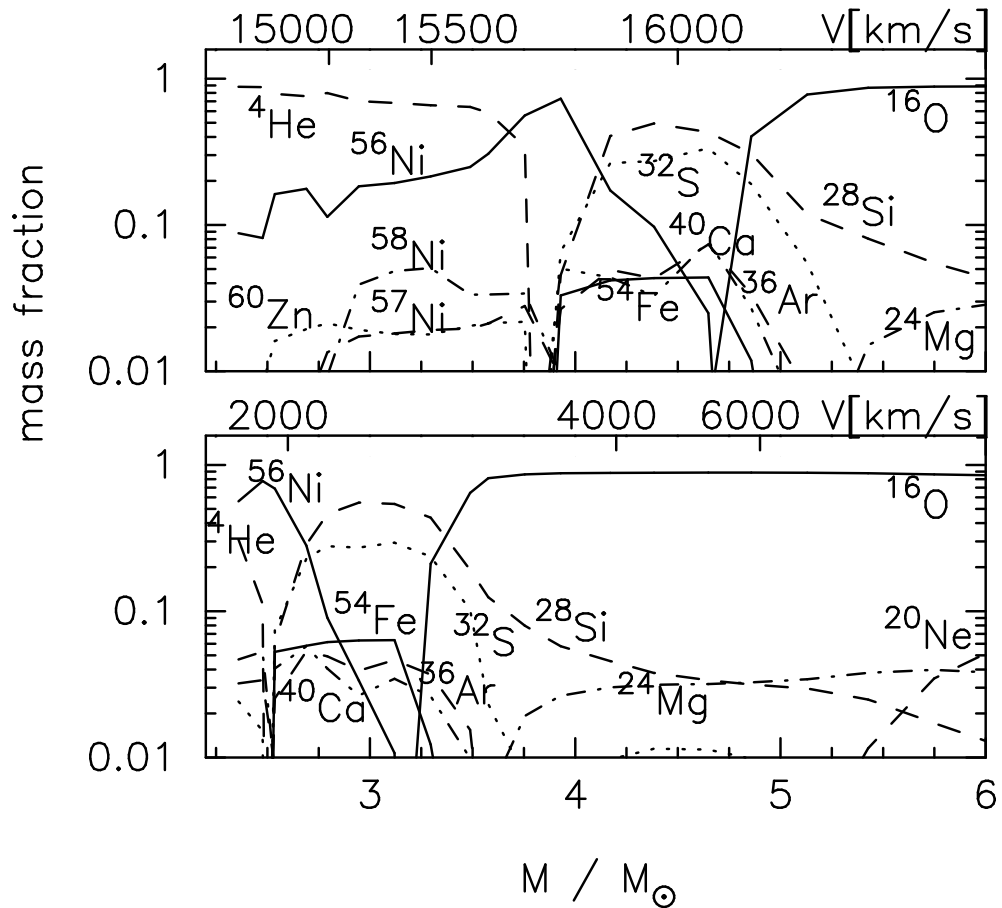


FIG. 1.— The isotopic composition of the ejecta of model C in the direction of the jet (upper panel) and perpendicular to the jet (lower panel). The ordinate indicates the initial spherical Lagrangian coordinate ( $M_r$ ) of the test particles (lower scale), and the final expansion velocities ( $V$ ) of those particles (upper scale).

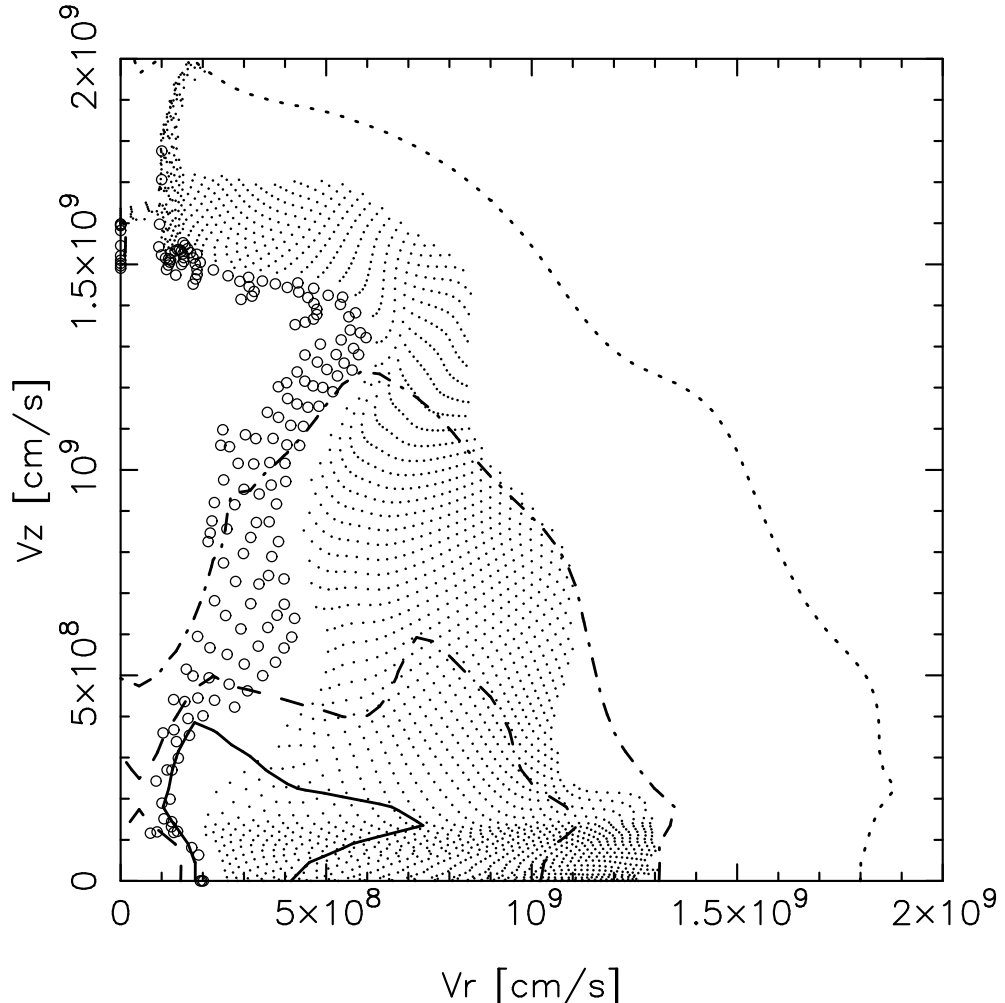


FIG. 2.— The distribution of  $^{56}\text{Ni}$  (open circles) and  $^{16}\text{O}$  (dots) of model C in the homologous expansion phase. The open circles and the dots denote test particles in which the mass fraction of  $^{56}\text{Ni}$  and  $^{16}\text{O}$ , respectively, exceeds 0.1. The lines are density contours at the level of 0.5 (solid), 0.3 (dashed), 0.1 (dash-dotted), and 0.01 (dotted) of the max density, respectively.

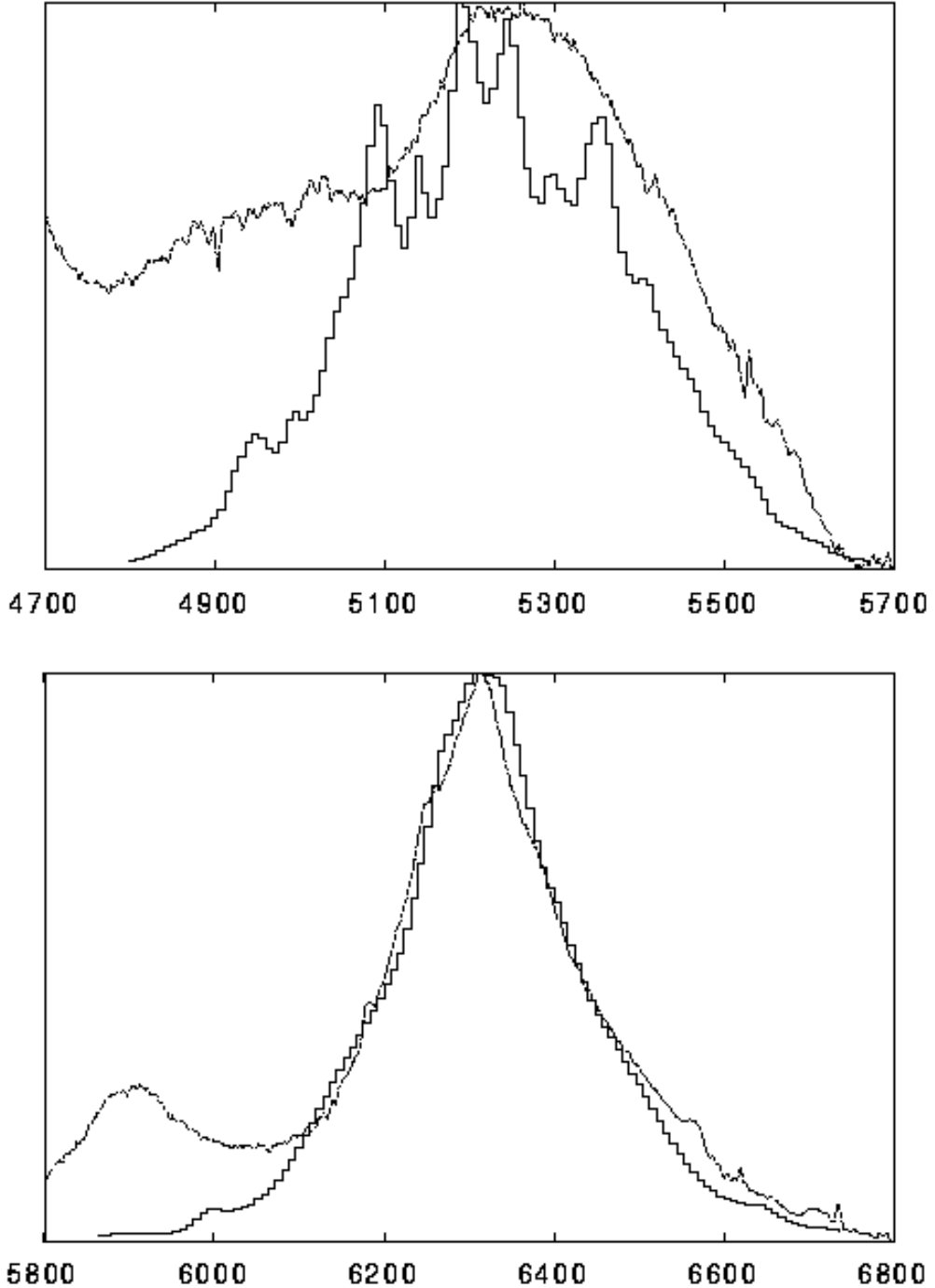


FIG. 3.— The profiles of the Fe-blend (upper panel) and of O I] 6300, 6363 Å (lower panel) for model C viewed at 15° from the jet direction (solid lines). The observed lines at a SN rest-frame epoch of 139 days are also plotted for comparison (dotted lines, Patat et al. 2000). The intensities of the strongest lines, normalized to O I 6300.3Å are: Fe II 5158.8Å: 0.207; Fe II 5220.1Å: 0.043; Fe II 5261.6Å: 0.139; Fe II 5273.3Å: 0.066; Fe II 5333.6Å: 0.099; Fe III 5270.4Å: 0.086; and OI 6363.8Å: 0.331.